Inference in conditioned dynamics through causality restoration

Alfredo Braunstein,^{1,2,3} Giovanni Catania,⁴ Luca Dall'Asta,^{1,2,3} Matteo Mariani,^{1,*} and Anna Paola Muntoni^{1,3}

¹DISAT, Politecnico di Torino, Corso Duca Degli Abruzzi 24, 10129 Torino

²Collegio Carlo Alberto, P.za Arbarello 8, 10122, Torino, Italy

³Italian Institute for Genomic Medicine, IRCCS Candiolo, SP-142, I-10060 Candiolo (TO), Italy

⁴Departamento de Física Téorica I, Universidad Complutense, 28040 Madrid, Spain

Computing observables from a conditioned dynamics is typically computationally hard, because, although obtaining independent samples efficiently from the unconditioned dynamics is usually feasible, generally most of the samples must be discarded (in a form of importance sampling) because they do not satisfy the imposed conditions. Sampling directly from the conditioned distribution is non-trivial, as conditioning breaks the causal properties of the dynamics which ultimately renders the sampling procedure efficient. One standard way of achieving it is through a Metropolis Monte-Carlo procedure, but this procedure is normally slow and a very large number of Monte-Carlo steps is needed to obtain a small number of statistically independent samples. In this work we propose an alternative method to produce independent samples from a conditioned distribution. The method learns the parameters of a generalized dynamical model that optimally describe the conditioned distribution in a variational sense. The outcome is an effective, unconditioned, dynamical model, from which one can trivially obtain independent samples, effectively restoring causality of the conditioned distribution. The consequences are twofold: on the one hand, it allows us to efficiently compute observables from the conditioned dynamics by simply averaging over independent samples. On the other hand, the method gives an effective unconditioned distribution which is easier to interpret. The method is flexible, and can be applied virtually to any dynamics. We discuss an important application of the method, namely the problem of epidemic risk assessment from (imperfect) clinical tests, for a large family of time-continuous epidemic models endowed with a Gillespie-like sampler. We show that the method compares favourably against the state of the art, including the soft-margin approach and mean-field methods.

I. INTRODUCTION

Let us denote by $\mathbb{P}[x]$ the probability distribution of trajectories x of a dynamical model. Given a (hidden) realization x^* , consider an observation \mathcal{O}^* sampled from a (known) conditional distribution $\mathbb{P}[\mathcal{O}|x^*]$. The scope of this work is to devise an efficient method to infer (as much as it is possible) information about x^* given the observation \mathcal{O}^* , in particular to be able to estimate averages over the posterior distribution

$$\mathbb{P}[\boldsymbol{x}|\mathcal{O}] = \mathbb{P}[\boldsymbol{x}] \, \mathbb{P}[\mathcal{O}|\boldsymbol{x}] \, \mathbb{P}[\mathcal{O}]^{-1} \,. \tag{1}$$

Although it might be generally feasible to sample efficiently from $\mathbb{P}[x]$, sampling from $\mathbb{P}[x|\mathcal{O}]$ is generally difficult. A naive approach is given by importance sampling, that consists in evaluating the average of a function f by first generating M independent samples x^1, \ldots, x^M from $\mathbb{P}[x]$ and then computing

$$\langle f \rangle \approx \frac{\sum_{\mu=1}^{M} f(\boldsymbol{x}^{\mu}) \mathbb{P}[\boldsymbol{x}^{\mu}] \mathbb{P}[\mathcal{O}|\boldsymbol{x}^{\mu}]}{\sum_{\mu=1}^{M} \mathbb{P}[\boldsymbol{x}^{\mu}] \mathbb{P}[\mathcal{O}|\boldsymbol{x}^{\mu}]}.$$
 (2)

Unfortunately, this method is impractical when observations deviate significantly from the typical case, as for the case in which $\mathbb{P}\left[\mathcal{O}|\boldsymbol{x}^{\mu}\right]$ becomes very small (or even zero), making the convergence to the true average value too slow.

^{*} matteo.mariani@polito.it

One reason for which sampling from $\mathbb{P}[x]$ is usually feasible is that the causal structure induced by the dynamical nature of the stochastic process can be exploited to efficiently generate trajectories. The *causal* property of the stochastic dynamics lies in the fact that the state of the system at a given time depends naturally (in a stochastic way) on states at previous times. For instance, when time is discretized in epochs $0, \Delta t, 2\Delta t, ...$, this property implies that the distribution of trajectories of the stochastic dynamics assumes the following simple form:

$$\mathbb{P}\left[\boldsymbol{x}\left(0\right),...,\boldsymbol{x}\left(k\Delta t\right)\right] = \mathbb{P}\left[\boldsymbol{x}\left(0\right)\right] \prod_{\ell=1}^{k} \mathbb{P}\left[\boldsymbol{x}\left(\ell\Delta t\right)|\boldsymbol{x}\left(0\right),...,\boldsymbol{x}\left(\left(\ell-1\right)\Delta t\right)\right],\tag{3}$$

that further simplifies in the memory-less case (Markov), in which $\mathbb{P}[\boldsymbol{x}(\ell\Delta t)|\boldsymbol{x}(0),...,\boldsymbol{x}((\ell-1)\Delta t)] = \mathbb{P}[\boldsymbol{x}(\ell\Delta t)|\boldsymbol{x}((\ell-1)\Delta t)]$. If one also assumes, like in most common agent-based models, that the dynamical process also satisfies a spatial conditional independence property, namely that

$$\mathbb{P}[\boldsymbol{x}(\ell\Delta t)|\boldsymbol{x}(0),...,\boldsymbol{x}((\ell-1)\Delta t)] = \prod_{i=1}^{N} \mathbb{P}[x_{i}(\ell\Delta t)|\boldsymbol{x}(0),...,\boldsymbol{x}((\ell-1)\Delta t)], \tag{4}$$

then it follows that efficient sampling from $\mathbb{P}[x]$ is possible. The fact that it is difficult to sample from $\mathbb{P}[x|\mathcal{O}]$ can be understood as a consequence of *causality breaking*, due to the addition of the extra information \mathcal{O} , which in simple terms means that $\mathbb{P}[x|\mathcal{O}]$ can no longer be interpreted (at least intuitively) as the distribution of a dynamical process.

The approach proposed here, called Causal Variational Approach (CVA), aims at providing a variational approximation of the posterior distribution $\mathbb{P}[\boldsymbol{x}|\mathcal{O}]$, for which causality features are restored and from which independent samples can be efficiently generated. Even though, indeed, it is always possible to rewrite any probability distribution Q in a causal form as $Q(\boldsymbol{x}_1,\ldots,\boldsymbol{x}_T)=\prod_{t=1}^Tq_t(\boldsymbol{x}_t|\boldsymbol{x}_{t-1},\ldots\boldsymbol{x}_1)$, it is not possible in general to calculate efficiently (and to sample from) each factor. We propose to approximate $\mathbb{P}[\boldsymbol{x}|\mathcal{O}]\approx Q(\boldsymbol{x})$ by giving a simple form for each q_t which resembles the original transition rates of the prior distribution $\mathbb{P}[\boldsymbol{x}]$. For example, we preserve the conditional independence of individual variable states at a given time, namely the factorization of the transition rates in space: $q_t(\boldsymbol{x}_t|\boldsymbol{x}_{t-1},\ldots,\boldsymbol{x}_1)=\prod_i q_t^i(x_t^i|\boldsymbol{x}_{t-1},\ldots,\boldsymbol{x}_1)$. Each factor, moreover, might depend only on a restricted (local) set of variables, and it is natural to preserve this dependence. Note that if the prior is Markovian and the condition is time-factorized, $\mathbb{P}[\mathcal{O}|\boldsymbol{x}]=\prod_{t=1}^T\mathbb{P}[\mathcal{O}_t|\boldsymbol{x}_t]$ then it is easy to show that the posterior distribution is also Markovian, $\mathbb{P}[\boldsymbol{x}_t|\boldsymbol{x}_{t-1},\ldots,\boldsymbol{x}_1|\mathcal{O}]=\mathbb{P}[\boldsymbol{x}_t|\boldsymbol{x}_{t-1},\mathcal{O}]$. It is then natural to extend this property to the approximating rates, $q_t^i(x_t^i|\boldsymbol{x}_{t-1},\ldots,\boldsymbol{x}_1)=q_t^i(x_t^i|\boldsymbol{x}_{t-1})$ effectively restoring causality features of the unconditioned process.

The Causal Variational Approach is rather general and flexible, as it can be applied to a large class of dynamical models (including discrete and continuous time and space models, both with memory and memory-less). After presenting the CVA in a general setting, its main features will be discussed exploiting a conditioned random walk as a toy model. Then, an application to the important problem of epidemic inference and risk assessment on dynamic contact networks is developed and analyzed in detail.

II. THE CAUSAL VARIATIONAL APPROACH

The method is based on approximating the original constrained process by introducing an effective unconstrained causal process that is naturally consistent with the observations.

Let $Q_{\theta}(x)$ be the probability distribution of a generalized dynamics, parametrized by the vector θ of parameters. The best approximation to $\mathbb{P}[x|\mathcal{O}]$ (in a precise variational sense) can be obtained by observing that Eq.(1) can be interpreted as a Boltzmann distribution $Z^{-1} \exp[-H(x)]$ with $H(x) = -\log \mathbb{P}[x, \mathcal{O}]$ and $Z = \mathbb{P}[\mathcal{O}]$

and minimizing the corresponding variational free energy, i.e.

$$\mathcal{F}(Q_{\theta}) := \int d\boldsymbol{x} Q_{\theta}(\boldsymbol{x}) \log \frac{Q_{\theta}(\boldsymbol{x})}{\mathbb{P}[\boldsymbol{x}, \mathcal{O}]}$$
(5)

$$= \left\langle \log \frac{Q_{\theta}(\mathbf{x})}{\mathbb{P}[\mathbf{x}, \mathcal{O}]} \right\rangle_{Q_{\theta}}.$$
 (6)

This quantity can be estimated efficiently by sampling the distribution Q_{θ} . Note that $\mathcal{F}(Q_{\theta}) = D_{KL}(Q_{\theta}||\mathbb{P}[\boldsymbol{x}|\mathcal{O}]) - \log \mathbb{P}[\mathcal{O}]$ where D_{KL} is the Kullback-Leibler divergence. To optimize \mathcal{F} a gradient descent method can be employed, where the gradient can be also estimated by means of sampling, by simply noting that

$$\nabla_{\theta} \mathcal{F}(Q_{\theta}) = \left\langle \nabla_{\theta} \log Q_{\theta}(\mathbf{x}) \log \frac{Q_{\theta}(\mathbf{x})}{\mathbb{P}[\mathbf{x}, \mathcal{O}]} \right\rangle_{Q_{\theta}}.$$
 (7)

The crucial point in this estimation is that both Q_{θ} and $\mathbb{P}[\boldsymbol{x}, \mathcal{O}] = \mathbb{P}[\boldsymbol{x}] \mathbb{P}[\mathcal{O}|\boldsymbol{x}]$ have explicit expressions that, due to their causal structure, can be efficiently computed using rejection-free sampling, at difference with $\mathbb{P}[\boldsymbol{x}|\mathcal{O}]$ and $\mathbb{P}[\mathcal{O}]$ which typically do not.

In the Supplementary Information (Appendix D), we provide some technical details for the gradient descent process.

When a fixed point is reached, the corresponding distribution Q_{θ} gives an approximation of the posterior distribution $\mathbb{P}[\boldsymbol{x}|\mathcal{O}]$ for which the KL divergence between them is (locally) minimized, and that can be used to generate samples satisfying the constraints given by \mathcal{O} .

III. A TOY MODEL APPLICATION: CONDITIONED RANDOM WALK

A simple application of the method explained in the previous Section consists in generating an approximate probabilistic description for a conditioned random walk. A simple realization of the latter is a one-dimensional random walk, starting at site x(0) = 0 and forced to visit some given region of space during its temporal evolution. If the generating process is spatially homogeneous, the probability of every feasible trajectory x of length T is $\mathbb{P}[x] = 2^{-T}$ and, more importantly, every trajectory can be directly sampled by means of the causal generative process, a discrete-time Markov chain in which the conditional probability of a jump is $\mathbb{P}[x(t+1) = x(t) \pm 1 | x(t)] = 1/2$. Imposing the condition that the dynamics at time t has to travel inside a particular set $\mathcal{W}(t) \subseteq \mathbb{Z}$, the posterior probability of a trajectory x can be written as

$$\mathbb{P}\left[\boldsymbol{x}|\mathcal{W}\right] = \frac{\prod_{t=1}^{T} \mathbb{I}[x\left(t\right) \in \mathcal{W}(t)]}{\sum_{\boldsymbol{y}} \prod_{t=1}^{T} \mathbb{I}[y\left(t\right) \in \mathcal{W}(t)]},\tag{8}$$

which can no longer be intuitively expressed as the result of a causal dynamical process. Within the framework provided by CVA, the transition probabilities can be generalized introducing site-dependent and time-dependent jump rates r_x^t , such that the posterior distribution can be approximated by the causal ansatz

$$Q_{\theta}(\mathbf{x}) = \prod_{t=0}^{T-1} \sum_{x} \left[r_x^t \delta_{x(t+1),x+1} + \left(1 - r_x^t \right) \delta_{x(t+1),x-1} \right] \delta_{x(t),x}, \tag{9}$$

with $\theta = \{r_x^t\}_{x=-T,...,T}^{t=1,...,T}$. The distribution Q_θ requires T(2T+1) parameters, where 2T+1 is the total number of sites that can be visited by realizations of the random walk. These parameters can be tuned using the CVA by minimizing the KL distance between Q_θ and the posterior distribution. Fig. 1(left) shows a set of realizations of an unbiased random walk (black paths). In Fig. 1(center), instead, several constrained realizations of the

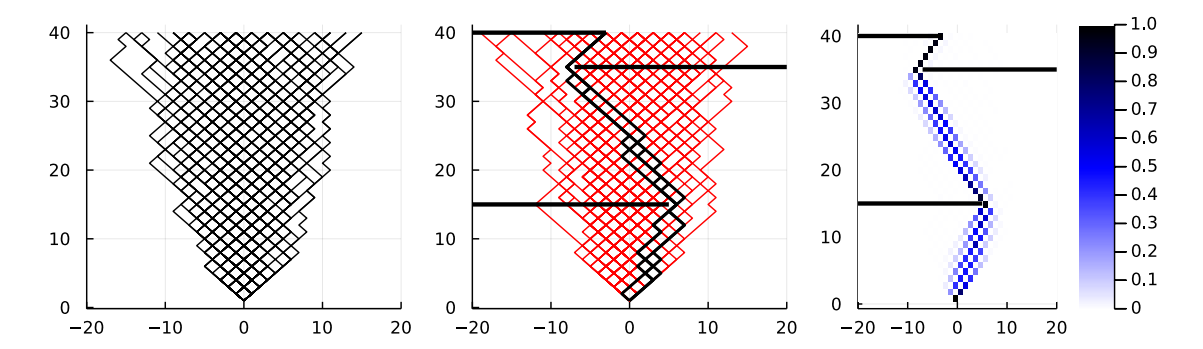


FIG. 1. Left: Unconditioned homogeneous Random Walk in on a one-dimensional lattice. Time is reported on the vertical axis (up to T=40) and the spatial coordinate x is on the horizontal axis. Center: Some RW trajectories are sampled from the unconditioned homogeneous distribution. The red ones do not satisfy the constraints, which require not to cross the horizontal lines. The black ones satisfy the constraints. The number of black lines is numerically calculated to be 10^{-6} less than the number of red lines. In other words, one every million trajectories satisfies the constraint if trajectories are sampled from the unconditioned distribution. Right. The distribution of the trajectories sampled from the CVA distribution. The colour of each pixel in the space-time indicates the probability for a trajectory to travel along that point.

dynamics are shown, where the trajectories were imposed not to cross three regions at some specific time steps (center, black horizontal barriers). Only a few trajectories satisfy the constraints (center, black paths) if compared with the possible unconstrained random walks in the left panel (the trajectories not satisfying the constraints are displayed as red paths in the central panel).

The posterior distribution Q_{θ} obtained sing the CVA is characterized by a very non-trivial spatio-temporal dependence of the rates r_x^t , which continuously vary between 0 and 1. The marginal distributions are represented, using a color scale, in Fig. 1 (right).

IV. APPLICATION TO EPIDEMIC INFERENCE

The Causal Variational Approach can be used to tackle some difficult problems emerging in the field of epidemic inference, such as the epidemic risk assessment from partial and time-scattered observations of cases, or the detection of the sources of infection. These problems have been recently addressed within a Bayesian probabilistic framework using computational methods inspired by statistical physics [1] or based on generative neural networks [2]. In particular, risk assessment from contact tracing data is of major importance for epidemic containment, because having access to an accurate measure of the individual risk can pave the way to effective targeted quarantine plans based on contact tracing devices. Here it is shown that the CVA can be a robust and effective tool for epidemic risk assessment and zero-patient inference.

Models and observations – According to the Bayesian framework, a prior probabilistic model $\mathbb{P}[x]$, a set of observations \mathcal{O} and the corresponding likelihood $\mathbb{P}[\mathcal{O}|x]$ have to be introduced. For the former, we consider a class of individual-based epidemic models describing the spreading process in a community of N individuals, interacting through a (possibly dynamic) contact network. The overall state of the system at time t (consisting of the state of each individual) is described by a vector $x(t) \in \mathcal{X}^N$, where \mathcal{X} is a finite set of possible health conditions (called compartments). The simplest, but already non-trivial, model of epidemic spreading is the discrete-time Susceptible-Infected (SI) model, in which $\mathcal{X} = \{S, I\}$ (corresponding to an individual being "susceptible" and "infected", respectively) where the only allowed transition occurs from state S to state I. More precisely, each time t, if an infected individual j is in contact with a susceptible individual i, the former can infect the latter (which moves into state I) with a transmission probability $\lambda_{ji}(t)$, sometimes called transmissivity. Since transmissions are independent, the individual transition probabilities are

$$\mathbb{P}\left[x_{i}\left(t+\Delta t\right)=S|\boldsymbol{x}\left(t\right)\right]=\delta_{x_{i}\left(t\right),S}\prod_{j\neq i}\left(1-\tilde{\lambda}_{ji}\left(t\right)\delta_{x_{j}\left(t\right),I}\right)$$
(10)

and $\mathbb{P}[x_i(t + \Delta t) = I | \boldsymbol{x}(t)] = 1 - \mathbb{P}[x_i(t + \Delta t) = S | \boldsymbol{x}(t)]$. A simple assumption is that time dependence only enters to describe the dynamic nature of the contact network (with $\tilde{\lambda}_{ji}(t) = 0$ if there is no contact between j and i at epoch t). More realistically, the transmission probability $\tilde{\lambda}_{ji}(t)$ should also depend on the current stage of infection of the infector j (e.g. presence/absence of symptoms) and thus mainly on the time elapsed since her own infection, making the epidemic dynamics non-Markovian.

Assuming transmission probabilities proportional to Δt in Eq.10 and defining transmission rates as $\lambda_{ij}(t) = \lim_{\Delta t \to 0^+} \tilde{\lambda}_{ij}(t) / \Delta t$, a continuous-time version of the SI model is obtained. Both for the discrete-time and continuous-time SI models, the history of the epidemic process can be fully specified by the "infection times" $\{t_i\}_{i=1}^N$ of all individuals; we conventionally set $t_i = 0$ if individual i is already infected at the initial time and $t_i = +\infty$ if i is never infected during the whole epidemic process. In terms of the trajectory vector $t := (t_1, \ldots, t_N)$, the probability pseudo density of an epidemic history can be generally written as

$$\mathbb{P}\left[\boldsymbol{t}\right] = \prod_{i} \left\{ \gamma \delta\left(t_{i}\right) + \left(1 - \gamma\right) \Lambda\left(\sum_{j \neq i} \mathbb{I}\left[t_{j} \leq t\right] \lambda_{ji}\left(t\right), t_{i}\right) \right\},\tag{11}$$

where γ denotes the probability of each individual to be a patient zero, and $\Lambda(f(t), b) = f(b) e^{-\int_{-\infty}^{b} f(t)dt}$ is the first-success distribution density¹ of an event with rate f(t). Hence, the quantity $\Lambda\left(\sum_{j\neq i} \mathbb{I}\left[t_{j} \leq t\right] \lambda_{ji}(t), t_{i}\right)$ is the probability density associated with the infection, at time t_{i} , of individual i by one of its infectious contacts at previous times.

In addition to the prior epidemic model, a set of observations has to be defined. In real epidemics, observations mirror the outcomes of medical tests, namely the state of an individual i at time t. For the sake of simplicity we define an auxiliary variable $r \in \{+,-\}$ (positive or negative test, respectively), such that each observation can be encoded as a triplet (i,t,r). Given the stochastic nature of clinical tests, we assume that the outcome r of a test performed on individual i at time t obeys a known conditional distribution law $\mathbb{P}[r|t_i]$ where t_i represents the infection time of individual i. When medical tests are affected by uncertainty, i.e. there exist a non-zero false positive and false negative rates of the diagnostic tests, the conditional probability states

$$\mathbb{P}[r = +|t_i| = (1 - p_{FNR}) \mathbb{I}[t_i \le t] + p_{FPR} \mathbb{I}[t_i > t]$$
(12a)

$$\mathbb{P}[r = -|t_i| = p_{FNR} \mathbb{I}[t_i \le t] + (1 - p_{FPR}) \mathbb{I}[t_i > t]$$
(12b)

For a population undergoing M individual test events, the set \mathcal{O} of observations is then identified with the set of triplets $(i^{\mu}, t^{\mu}, r^{\mu})$ for $\mu = 1, \dots, M$.

Given a realization of an epidemic model defined on a contact network, and the (possibly noisy) observation of the states of a subset of the individuals (at possibly different times), the epidemic risk assessment problem consists of estimating the epidemic risk, i.e. the risk of being infected, of the unobserved individuals at some specific time. In practice, it amounts to computing marginal probabilities from the posterior distribution. For the SI model, it can be computed as

$$\mathbb{P}\left[x_{i}\left(t\right) = I|\mathcal{O}\right] = \int d\mathbf{t}\mathbb{I}\left[t_{i} \leq t\right]\mathbb{P}\left[\mathbf{t}|\mathcal{O}\right]$$
(13)

¹ When $\int_{-\infty}^{b} \Lambda\left(f,t\right) dt < 1$, it means that there is a non-zero probability of the individual remaining susceptible. In that case, we will formally assign the defect mass $1 - \int_{-\infty}^{\infty} \Lambda\left(f,t\right) dt$ to $t = \infty$.

where $\int dt$ denotes the integral over all infections times t_1, \ldots, t_N .

A richer epidemic model, that is often used as a basis to develop more realistic ones (see e.g. Refs [3]), is the SEIR model, which contains also Exposed (E) and Recovered (R) states, i.e. $\mathcal{X} = \{S, E, I, R\}$, with the only allowed transitions being $S \to E$ (representing the contagion event), $E \to I$, $I \to R$, the latter two transition occurring for each individual independently of the others, with rates ν_i and μ_i . The previous representation in terms of the times where individual transitions occur can be straightforwardly generalized to the SEIR model, as well as the definition of observations from clinical tests and that of an individual risk measure (see Appendix B for additional details).

The Causal Variational Approach requires to generalize the prior probabilistic model in order to account for observational constraints. Here it is done by defining generalized versions of the infection rates $\lambda_i(t)$ and the zero-patient probabilities γ_i , and introducing a self-infection rate $\omega_i(t)$ for each individual i. As both $\lambda_i(t)$ and $\omega_i(t)$ are functions of time, an additional parametrization is necessary for computational purposes. Then, the trial distribution Q_{θ} is optimized with respect to the full set of parameters θ . Even in the simple case where the infection rates are uniform, the trial distribution computed at the minimum of the KL divergence is expected to have non-trivial time dependencies on the infection rates and self-infection probabilities, in such a way to take into account the effect of the observation constraints (a simple scenario with only two individuals that allows for an analytic treatment is presented in Appendix A) We refer further to Appendices C- E for a more detailed discussion on how the parametrization and the gradient descent are implemented.

Performances on synthetic networks – The performance of the CVA in reconstructing epidemic trajectories can be tested by measuring its ability in classifying the state of the unobserved individuals based on their predicted risk. The results are directly compared with those obtained using other inference techniques previously proposed in the literature, such as a Belief Propagation based method (sib) [1], a Soft Margin method (soft) adapted from [4], and simple heuristic methods based on Mean Field equations (MF) [1] or on sampling (heu). A description of the implementation of the different methods used for comparison is provided in Appendix G. For the sake of simplicity, we considered SI epidemic processes on proximity graphs, i.e. random graphs generated by proximity relationships between N individuals randomly distributed on a two-dimensional square region (see Appendix H for a definition). The set \mathcal{O} is composed of the observed states of randomly chosen individuals at a fixed time $t_{\rm obs}$. The observations have a false negative rate $p_{FNR} > 0$. The comparison between different inference methods is made by ranking the individual marginal probability of being in state I at a chosen time t^* and building the corresponding receiving operating characteristic (ROC) curve [5]. The AUC (area under the ROC curve) at a time t^* is an indicator of the accuracy of the method in reconstructing the state of the system at that time. The AUC at initial time ($t^* = 0$, patient-zero problem) and at the final time ($t^* = T$, risk assessment) are shown in Figure 2 as function of the performed number of observations. As expected, the performances of all methods increase on average if the number of observations (at time T) is increased. The results obtained with CVA are very close to those of the best performing methods (cau, sib and soft) in a large part of the region under study; in particular, they are comparable with those from the SoftMargin method, which in network instances with a small number of individuals is expected to be almost exact.

To further investigate the performances of the CVA against other state-of-the-art techniques, the risk assessment analysis was performed on a dynamic contact network instance, with realistic features, generated using the spatio-temporal model in Ref. [6] (see Appendix H). The epidemic realizations are generated using a SI model, for which the state of a given fraction of individuals is observed. A measure of the individual risk is computed, on a daily basis, according to all three different methods (cau, sib, soft) and the corresponding AUC is shown, as function of time (in days), in Figure 3. The left and the right panels depict the behavior of this measure when considering two slightly different observation protocols: in the left panel observations are performed at the final time T and nodes are observed according to a uniform distribution; in the right panel observation times are uniformly randomly extracted in the interval [1,T] and observations are biased towards tested-positive outcomes to mimic a realistic scenario where symptomatic, i.e. infected individuals, are more likely tested than susceptible ones. The CVA outperforms the Soft Margin-based method (soft) in both scenarios, and it turns out to be more robust than Belief Propagation (sib) with respect to changes in the observation protocol.

Hyperparameters Inference – In the previous numerical experiments, the parameters of the SI model used to generate the observations, i.e. the (homogeneous) infection rate λ and the probability of being the zero

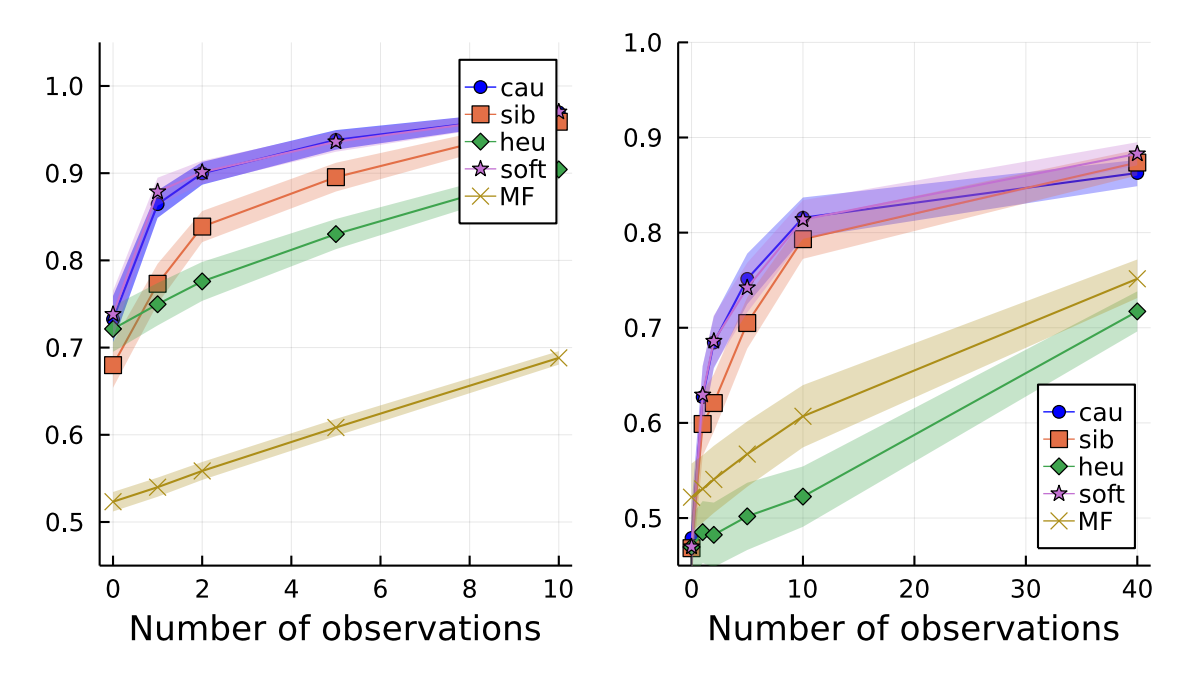


FIG. 2. Comparison among several inferential techniques as function of the number of observations for the risk assessment problem at time T (left) and for the patient-zero problem (right). The simulated contact graph is of proximity type with density 2.1/N. The following parameters are kept fixed: the total number of individuals N=50, the probability of being the zero patient $\gamma=1/N$, and the infection rate $\lambda=0.1$. For each epidemic realization we perform inference for an increasing number of observations at time T (here $p_{FNR}=0$). Shaded areas indicate the error on the averages computed over 60 different instances.

patient γ , are assumed to be known. These parameters enter in the Causal Variational Approach formalism as hyperparameters of the prior distribution. If these hyperparameters are not assumed to be known, the CVA can be used to estimate them from a sufficiently large number of observations. The quality of the inference is shown in Figure 4, where the numerical value of the attained minimum of the KL divergence D_{KL} is plotted using a color-scale for a grid of values of the hyperparameter space (λ, γ) . The region attaining the lowest values also contains the pair of true hyperparameter values (λ^*, γ^*) . The variational nature of the CVA becomes more visible when plotting, as oriented paths, the sequential values of KL divergence obtained starting from random points in the (λ, γ) plane and performing the gradient descent learning process (orange paths in Fig. 4). A detailed discussion about how to infer hyperparameters using gradient descent is provided in Appendix F.

Model reduction — For viral diseases with sufficiently known transmission mechanisms, agent-based modeling using discrete-state stochastic processes has proven useful to build large-scale simulators of epidemic outbreaks and design containment strategies [6, 7]. Such mathematical models are much more complex than the SI model analysed previously, as they need to include additional specific features of real-world diseases. In particular, models may assume different infected states, characterized by a different capability of transmitting the virus and diverse sensitivity to diagnostic tests. Another important feature that can emerge from realistic transmissions is that individuals can stop being infectious, even before recovering from the infected state, because of a decay of their viral load. These ingredients can be effectively included in the SI and SEIR models by introducing time-dependent infection rates, which is a natural assumption in the framework of the Causal Variational Approach. This property makes the latter a very suitable inference method to approximate unknown and possibly complex generative epidemic processes using classes of simpler probabilistic models. A simple test of such a potentiality is provided by the following example. We generate several epidemic realizations with a SEIR prior model and we compare the quality of the inference obtained by the Causal Variational Approach when (i) the SEIR model is

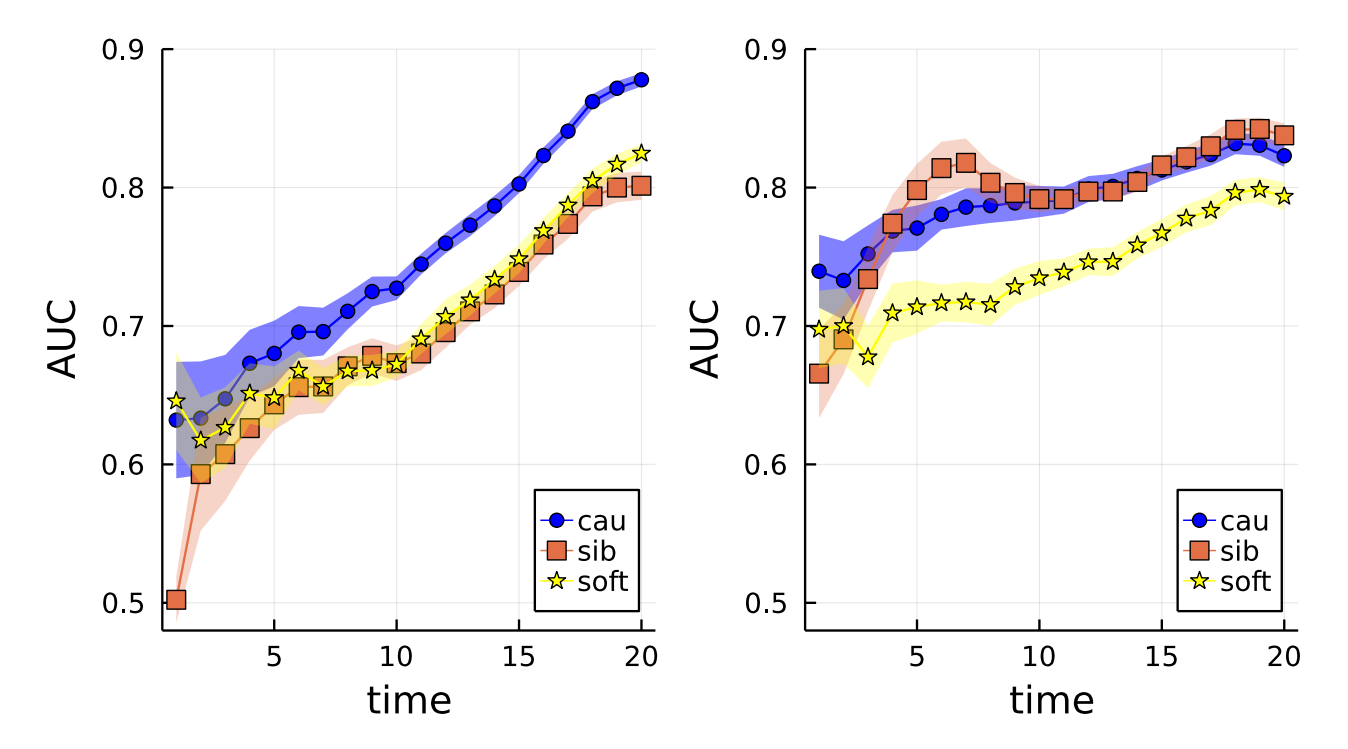


FIG. 3. AUC associated with the prediction of the infected individuals, for the Causal Variational Approach (cau), Belief Propagation (sib) and SoftMargin (soft), as a function of time during the epidemic propagation of a SI model ($\lambda=0.15$) on several instances of dynamic contact network generated using the spatio-temporal model in Ref. [6]. In the left panel the unique observation time $t_{\rm obs}$ coincides with the last time of the dynamic T=20, while in the right panel observation times are extracted uniformly in the range [1,T]; at each observation time $t_{\rm obs}$, infected nodes are observed with a biased probability equal to $1.1 \times N_I (t_{\rm obs})/N$ where $N_I (t_{\rm obs})$ is the number of infected individuals at time $t_{\rm obs}$ and N=904 is the total number of individuals.

also used as an ansatz for the posterior distribution and (ii) when the posterior distribution is approximated with a simpler probabilistic model, such as the SI model. If the parameters of the generative SEIR model are known, the hyperparameters of the SEIR posterior are also known. The corresponding results (green diamonds) for the AUC as function of time on a proximity graph are displayed in Fig. 5(left). Otherwise, the hyperparameters of the SEIR posterior can be also inferred by means of the CVA (blue circles). Finally, the ansatz for the posterior distribution can be simplified to a SI model, and the corresponding hyperparameters can be inferred as well within the CVA (red squares). The overall quality of the inference depends on the possibly different regimes of information contained in the observations. Strikingly, when the generative model is not known, the results from SEIR-based and SI-based inference are always very close to each other. For a sufficiently large number of observations such results are also close to those obtained with the SEIR posterior and known hyperparameters.

From a generative perspective, the inferred hyperparameters can be also interpreted as the epidemic parameters of some prior model, from which epidemic realizations can be sampled. It is natural to ask what are the statistical properties of such generative processes compared to the original one, from which the observations were sampled. Figure 5 also shows, in two different regimes, the average number of infected individuals as a function of time estimated from the original SEIR prior model (green diamond), the SEIR prior model with inferred hyperparameters (blue circles) and the SI prior model with inferred hyperparameters (red squares). The average number of infected individuals computed over the realizations from which the observations are sampled is also displayed (black line). The regimes shown in Fig. 5 correspond to unbiased observations (center panel, for $\lambda = 0.3$), and to observations preferentially sampled from large outbreaks (right panel, for $\lambda = 0.15$). Although

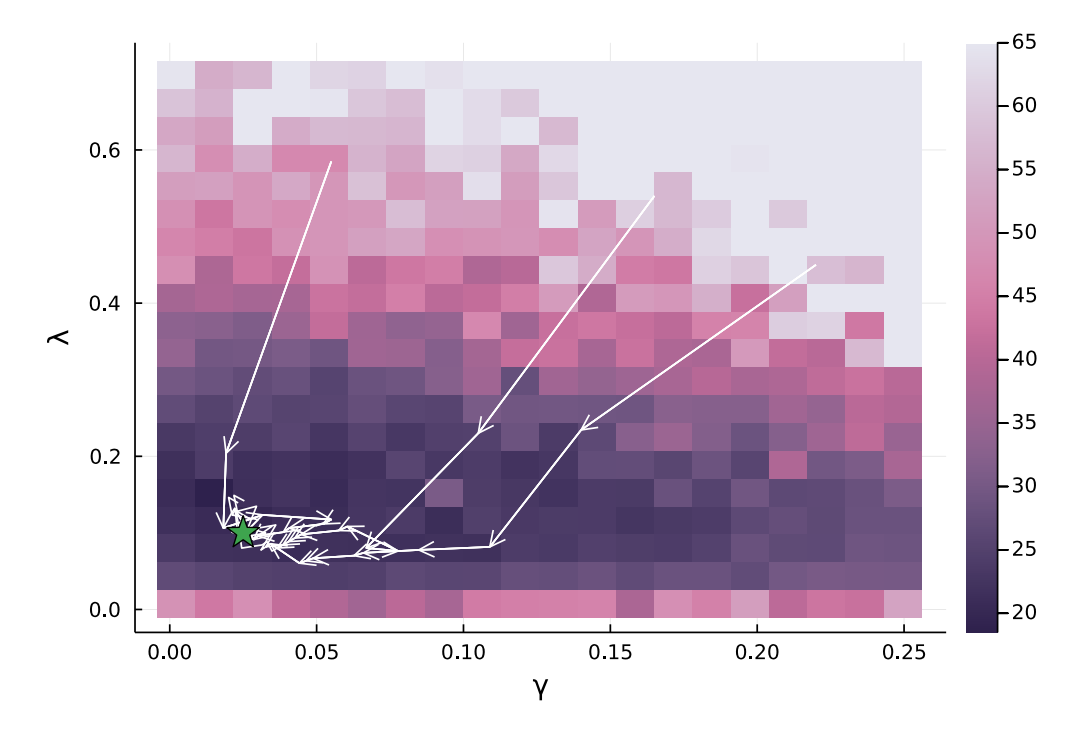


FIG. 4. Heat map of the free energy $(-\log \mathbb{P}(\mathcal{O}))$ as function of the hyperparameters of the SI model. In a proximity graph with N=50 individuals and density $\rho=2/N$, an epidemic instance was generated with zero-patient probability $\gamma^*=1/N$ and infection rate $\lambda^*=0.1$. After collecting a large number of observations $(n_{obs}=2N)$, an approximation of the free energy $-\log \mathbb{P}[\mathcal{O}]$ is calculated with the CVA for several values of λ and γ . As expected, the minimum of this function is close to the exact value (γ^*, λ^*) , which is represented with a star on the plot. The oriented paths (white arrows) represent the convergence towards the minimum of $-\log \mathbb{P}[\mathcal{O}]$ obtained performing a gradient descent algorithm over the hyperparameters starting from three different initial points in the plane (γ, λ) .

the discrepancy between the different curves is significant, the moderate difference between predictions obtained using SEIR and SI prior models with inferred hyperparameters suggests that model reduction is only a minor source of information bias.

V. CONCLUSIONS

Sampling from the posterior distribution of a conditioned dynamical process can be computationally hard. In this work, a novel computational method to accomplish this task, called the Causal Variational Approach, was put forward. The Causal Variational Approach is based on the idea of inferring the posterior with an effective, unconditioned, dynamical model, whose parameters can be learned by minimising a corresponding free energy functional.

An insight into the potential of the method is obtained analyzing a one-dimensional conditioned random walk in which some regions of space are forbidden. The CVA produces a generalised random walk process, with space-dependent and time-dependent jump rates, whose unconditioned realizations satisfy the imposed constraints. An application of greater practical interest concerns epidemic inference, in particular the risk assessment from partial and time-scattered observations. For simple stochastic epidemic models, such as SI and SEIR, taking place on contact networks of moderately small size, the CVA performs better or as good as the best methods currently available. Moreover, the variational nature of the method allows one to estimate the

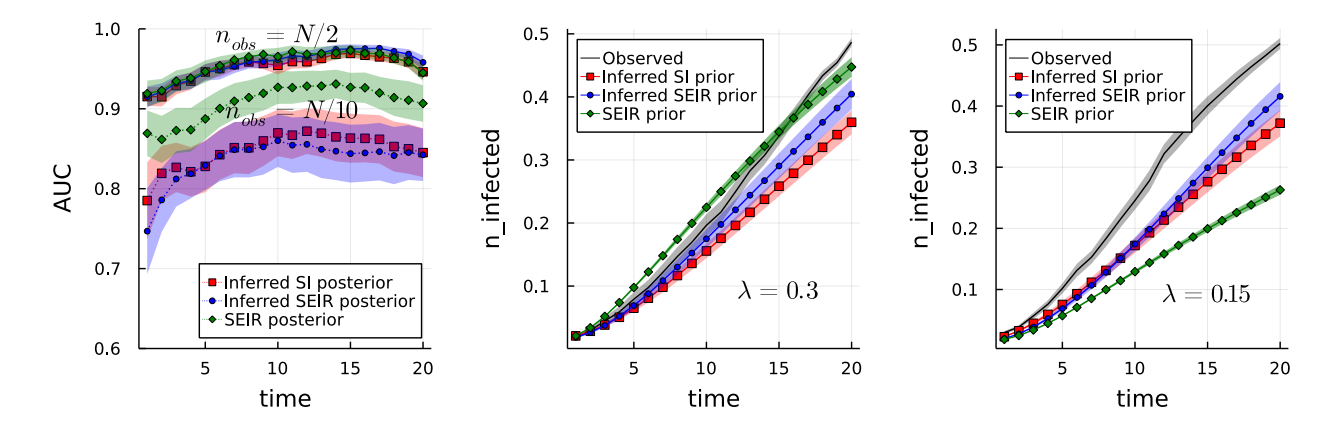


FIG. 5. Effects of model reduction on inferential performances and generative capabilities. The numerical experiments are performed on a proximity graph with N=100 individuals and density 2.2/N. The observed epidemic realizations are generated using a SEIR model with $\gamma=1/N$, $\lambda=0.3$ (left and center panels) and 0.15 (right panel), latency delay $\nu=0.5$ and recovery delay $\mu=0.1$. Left: Values of the AUC as function of time obtained using the CVA in two observation regimes (when the number of observations is $n_{obs}=N/10$ and $n_{obs}=N/2$), with the three different inferred posterior distributions: a SEIR model with known hyperparameters (green diamonds), a SEIR model with unknown hyperparameters (blue circles) and a SI model with unknown hyperparameters (red squares). Shaded areas represent the error around the average value, computed using 22 instances. Center-Right: The average fraction of infected individuals as a function of time estimated using the correct SEIR prior model (green diamonds), a SEIR prior with the inferred hyperparameters (blue circles) and a SI prior model with the inferred hyperparameters (red squares). The regimes shown correspond to unbiased observations (center, for $\lambda=0.3$), and to observations preferentially sampled from large outbreaks (right, for $\lambda=0.15$). The black curves represent the same quantity computed from the observed epidemic realizations. Shaded areas represent the error around the average value.

likelihood of the parameters of the original epidemic model that generated the observations, which enter the CVA in the form of hyperparameters. Since the CVA approximates the posterior distribution of the epidemic process by learning a set of generalised individual-based, time-dependent parameters, even with a rather simple ansatz for the epidemic model, such as an SI model, inference from observations coming from more complex epidemic processes can be performed. In fact, a generalised SI model with time-dependent infection rates and self-infection rates allows one to accommodate many features of real-world epidemic diseases, such as time-varying viral load and transmissivity, incubation and recovery. The performances of the Causal Variational Approach do not seem to suffer from model reduction from SEIR to SI, suggesting that simplified epidemic models could be effective for inference also in real-world cases. The Causal Variational Approach is very flexible and, employing sampling to perform estimates, it can be applied virtually to any dynamics for which the latter can be carried out efficiently. In particular, the method can thus be applied to inference problems involving recurrent epidemic processes, such as the SIS model [8] or other models with immunity decay over time.

^[1] Antoine Baker, Indaco Biazzo, Alfredo Braunstein, Giovanni Catania, Luca Dall'Asta, Alessandro Ingrosso, Florent Krzakala, Fabio Mazza, Marc Mézard, Anna Paola Muntoni, Maria Refinetti, Stefano Sarao Mannelli, and Lenka Zdeborová. Epidemic mitigation by statistical inference from contact tracing data. *Proceedings of the National Academy of Sciences*, 118(32):e2106548118, August 2021. Publisher: Proceedings of the National Academy of Sciences.

^[2] Indaco Biazzo, Alfredo Braunstein, Luca Dall'Asta, and Fabio Mazza. Epidemic inference through generative neural networks. *CoRR*, abs/2111.03383, 2021.

^[3] Cliff C Kerr, Robyn M Stuart, Dina Mistry, Romesh G Abeysuriya, Katherine Rosenfeld, Gregory R Hart, Rafael C

- Núñez, Jamie A Cohen, Prashanth Selvaraj, Brittany Hagedorn, et al. Covasim: an agent-based model of covid-19 dynamics and interventions. *PLOS Computational Biology*, 17(7):e1009149, 2021.
- [4] Nino Antulov-Fantulin, Alen Lančić, Tomislav Šmuc, Hrvoje Štefančić, and Mile Šikić. Identification of patient zero in static and temporal networks: Robustness and limitations. *Phys. Rev. Lett.*, 114:248701, Jun 2015.
- [5] Tom Fawcett. An introduction to ROC analysis. Pattern Recognition Letters, 27(8):861–874, June 2006.
- [6] Lars Lorch, William Trouleau, Stratis Tsirtsis, Aron Szanto, Bernhard Schölkopf, and Manuel Gomez-Rodriguez. A spatiotemporal epidemic model to quantify the effects of contact tracing, testing, and containment, 2020.
- [7] Robert Hinch, William JM Probert, Anel Nurtay, Michelle Kendall, Chris Wymant, Matthew Hall, Katrina Lythgoe, Ana Bulas Cruz, Lele Zhao, Andrea Stewart, et al. Openabm covid19 an agent-based model for non-pharmaceutical interventions against covid-19 including contact tracing. PLoS computational biology, 17(7):e1009146, 2021.
- [8] Ernesto Ortega, David Machado, and Alejandro Lage-Castellanos. Dynamics of epidemics from cavity master equations: Susceptible-infectious-susceptible models. *Phys. Rev. E*, 105:024308, Feb 2022.
- [9] Jeremy Bernstein, Yu-Xiang Wang, Kamyar Azizzadenesheli, and Animashree Anandkumar. signSGD: Compressed Optimisation for Non-Convex Problems. In Proceedings of the 35th International Conference on Machine Learning, pages 560–569. PMLR, July 2018. ISSN: 2640-3498.

Appendix A: Exact posterior distribution of a SI model with two individuals and one observation

A simple but instructive example to understand how the Causal Variational Approach can obtain good approximations of the posterior distribution in epidemic processes is provided analyzing the case of a continuous-time SI model with only two individuals, A and B. In this example, we assume that (i) both individuals have the same probability γ of being initially infected and (ii) they can infect each other, if infectious, with the same constant infection rate λ . A graphical representation of the role played by these parameters is shown in Figure 6 (left).

Suppose an individual A is observed at time $t_{\rm obs} = T$ in the infected state (e.g., performing a clinical test), then there are two possible explanations for such an observation: either A was already infected at time t = 0 or A got infected by B at a time t < T. In both cases, the observation forces the dynamics to satisfy the constraint that A is in state I at time T. One can speculate that the observation breaks the causality property of the dynamics because a constraint set on the future (time T) affects the dynamics at previous times. If, in fact, A is not the zero patient, then B must have infected A at previous times. The effective posterior infection rate from B to A, therefore, must diverge when $t \to T$.

The epidemic trajectory can be described defining $\mathbf{t} := (t_A, t_B)$, where t_A and t_B are the infection times of the two individuals. In terms of \mathbf{t} , the SI prior distribution can be written as

$$\mathbb{P}[t] = \begin{cases} \gamma^2 & t_{A} = t_{B} = 0, \\ (1 - \gamma)^2 & t_{A} = t_{B} = \infty, \\ \gamma (1 - \gamma)e^{-\lambda t}\lambda & t_{A} = t \text{ and } t_{B} = 0, \text{ or } t_{A} = 0 \text{ and } t_{B} = t, \\ 0 & \text{otherwise.} \end{cases}$$
(A1)

This prior probability distribution² is normalized, indeed

$$\gamma^{2} + 2\gamma(1-\gamma)\lambda \int_{0}^{\infty} e^{-\lambda t} dt + (1-\gamma)^{2} = \gamma^{2} + 2\gamma(1-\gamma) + (1-\gamma)^{2} = 1.$$
 (A2)

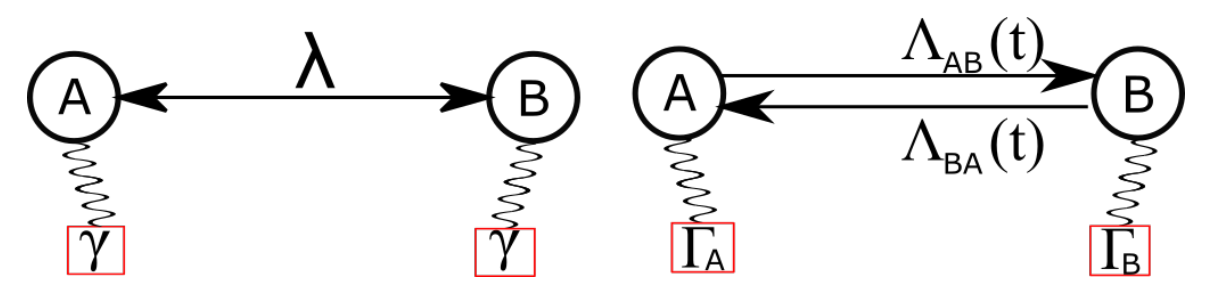


FIG. 6. Schematic representation of the role played by the epidemic parameters in a SI model with two individuals. Left: In the original SI model, individuals A and B have the same probability γ of being initially infected, and the same infection rate λ . Right: in the prior SI model used to compute the posterior by means of the CVA, γ are replaced by possibly different probabilities Γ_A , Γ_B and the infection rate λ is replaced by time-dependent rates $\Lambda_{AB}(t)$, $\Lambda_{BA}(t)$. These parameters are inferred by minimizing the KL divergence in Eq. (5).

² There is a little abuse of notation. $p_{AB}(0,0)$ and $p_{AB}(\infty,\infty)$ are probabilities, while the other term is a density of probability. The point is that the events of having two zero patients or no infections have finite probability, while the event of having a particular infection time is infinitesimal in probability and must be integrated over time.

The observation of the state of individual A implies that

$$\mathbb{P}[\mathcal{O}|\mathbf{t}] = \begin{cases} 0 & \text{if } t_{\mathcal{A}} > T\\ 1 & \text{otherwise.} \end{cases}$$
 (A3)

The posterior distribution $\mathbb{P}[t|\mathcal{O}]$ can be computed using Bayes theorem as

$$\mathbb{P}[t|\mathcal{O}] = \frac{\mathbb{P}[t]\mathbb{P}[\mathcal{O}|t]}{\mathbb{P}[\mathcal{O}]}$$
(A4)

$$= \frac{1}{\mathbb{P}[\mathcal{O}]} \begin{cases} \gamma^2 & t_{\mathcal{A}} = t_{\mathcal{B}} = 0\\ \gamma (1 - \gamma) e^{-\lambda t_{\mathcal{A}}} \lambda & 0 < t_{\mathcal{A}} < T \text{ and } t_{\mathcal{B}} = 0\\ \gamma (1 - \gamma) e^{-\lambda t_{\mathcal{B}}} \lambda & t_{\mathcal{A}} = 0\\ 0 & \text{otherwise.} \end{cases}$$
(A5)

where the denominator is given by

$$\mathbb{P}[\mathcal{O}] = \gamma^2 + \int_0^T dt_{\rm A} \, p_{\rm AB}(t_{\rm A}, 0) + \int_0^\infty dt_{\rm B} \, p_{\rm AB}(0, t_{\rm B}) =$$
(A6)

$$= \gamma^2 + \gamma(1 - \gamma) \left(2 - e^{-\lambda T}\right). \tag{A7}$$

It is convenient to compute the posterior probability that individuals are infected at the initial time given the observation \mathcal{O} ,

$$\mathbb{P}[t_{\mathcal{A}} = 0|\mathcal{O}] = \frac{\gamma}{\gamma^2 + \gamma(1 - \gamma)(2 - e^{-\lambda T})} =: \Gamma_{\mathcal{A}}$$
(A8)

$$\mathbb{P}[t_{\rm B} = 0|\mathcal{O}] = \frac{\gamma + (1 - \gamma)\left(1 - e^{-\lambda T}\right)}{\gamma + (1 - \gamma)\left(2 - e^{-\lambda T}\right)} =: \Gamma_{\rm B}$$
(A9)

For both individuals, non causal effects arise as the infection probabilities at time 0 also depend on the infection rate λ and on the observation time T. Moreover, the expressions of $\Gamma_{\rm A}$, $\Gamma_{\rm B}$ are different because the observation on A has broken the symmetry between the two individuals.

It is also possible to compute the posterior probability that individual B is infected at time t, which implies that A is initially infected, namely

$$\Lambda_{AB}(t) := \lim_{\epsilon \to 0} \frac{\mathbb{P}[t_B = t + \epsilon, t_A = 0 | \mathcal{O}]}{\mathbb{P}[t_B > t, t_A = 0 | \mathcal{O}]} = \lim_{\epsilon \to 0} \frac{\gamma(1 - \gamma)e^{-\lambda(t + \epsilon)}\lambda}{\gamma(1 - \gamma)e^{-\lambda t}} = \lambda$$
(A10)

and the posterior probability that individual A is infected at time t by B, i.e.

$$\Lambda_{\text{BA}}(t) := \lim_{\epsilon \to 0} \frac{\mathbb{P}[t_{\text{A}} = t + \epsilon, t_{\text{B}} = 0 | \mathcal{O}]}{\mathbb{P}[t_{\text{A}} > t, t_{\text{B}} = 0 | \mathcal{O}]}$$

$$= \lim_{\epsilon \to 0} \frac{\gamma(1 - \gamma)e^{-\lambda(t + \epsilon)}\lambda}{\gamma(1 - \gamma)\lambda \int_{t}^{T} e^{-\lambda s} ds} = \lim_{\epsilon \to 0} \frac{e^{-\lambda(t + \epsilon)}\lambda}{(e^{-\lambda t} - e^{-\lambda T})} = \frac{\lambda e^{-\lambda t}}{e^{-\lambda t} - e^{-\lambda T}}.$$
(A11)

The two quantities differ because here the observation forces individual B to infect A before the observation time $t_{\text{obs}} = T$, causing the infection rate $\Lambda_{\text{BA}}(t)$ to diverge when $t \to T$.

The exact posterior distribution (A5) can be expressed in the form of a generalized SI model with asymmetric probabilities $\Gamma_{\rm A}$ and $\Gamma_{\rm B}$ that the individuals are already infected at the initial time and time-dependent infection

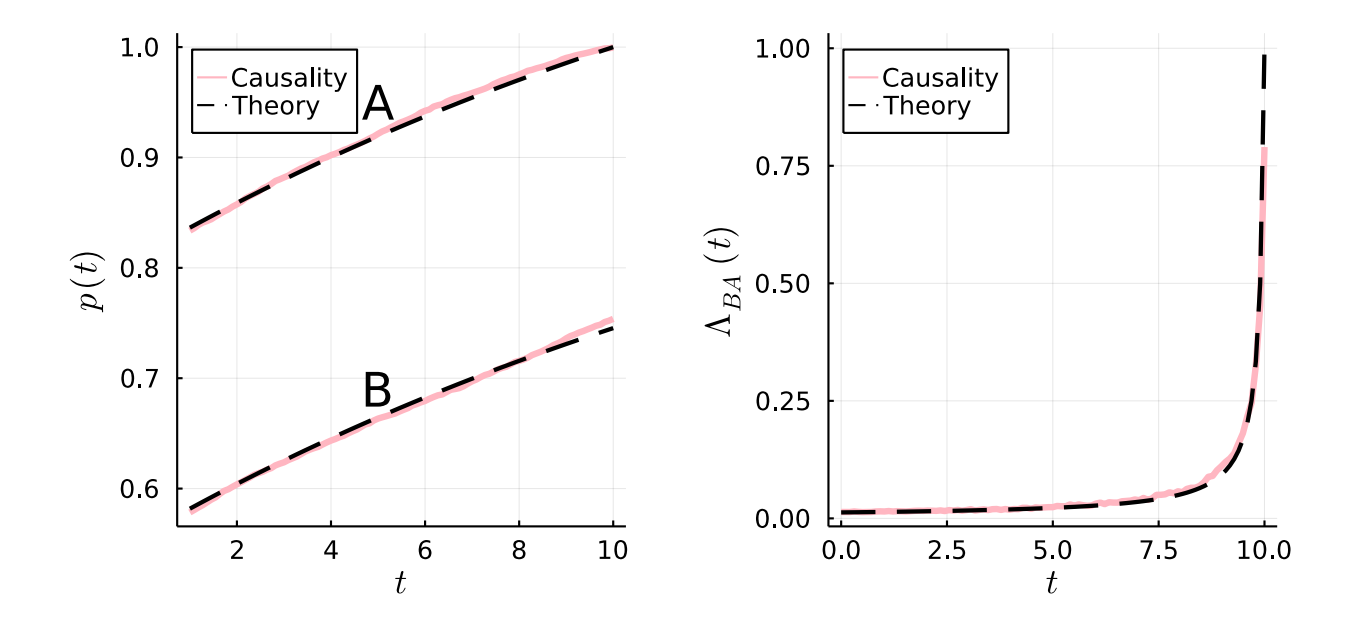


FIG. 7. . Comparison between the exact calculations (dashed black lines) and results obtained using the CVA (red lines) for a SI model ($\lambda=0.05$ and $\gamma=1/2$) with two individuals A and B, where A is observed infected at the final time T=10. Left: Marginal probabilities of being infected for individuals A and B as function of time. Due to the observation on A at time T, the two marginals are different: in particular, individual A's marginal reaches 1 at time T in such a way to be consistent with the observation. Right: Effective infection rate $\Lambda_{\rm BA}(t)$ as function of time. The divergence is due to the observation on individual A at time T.

rates $\Lambda_{AB}(t)$ and $\Lambda_{BA}(t)$. A schematic representation of the role played by these parameters as compared with the ones of the original SI model is provided in Fig. 6 (right). Such a generalized SI model can be used as an ansatz distribution Q_{θ} in the CVA. The minimum of the corresponding free energy is obtained when the generalized parameters Γ_{A} , Γ_{B} , $\Lambda_{AB}(t)$ and $\Lambda_{BA}(t)$ assume exactly the form derived above in Eqs. (A8),(A9),(A10) and (A11). It follows that the CVA provides a formally exact solution to the inference problem under study. This is shown in Figure 7, where the exact solution of the model is compared with the solution found using the CVA.

Appendix B: Probabilistic description of the SEIR model with observations

The Susceptible-Exposed-Infected-Recovered (SEIR) model is a generalization of the SI model in which incubation (E) and recovery (R) are included. The only allowed transitions are $S \to E$, $E \to I$, $I \to R$. A transmission event by an infected individual j brings a susceptible individual i into the E state with a rate λ_{ji} , then the transition to I occurs independently of the rest of the system with rate ν_i . Finally, an infected individual i recovers, again independently of the others, with rate μ_i . In this model, the trajectory of the epidemic process is fully specified by three times: $t_i^E \leq t_i^I \leq t_i^R \in \mathbb{R}_{\geq 0}$, representing the times in which individual i enters the states E, I and R, respectively. For an individual infected at time zero we have $t_i^E = t_i^I = 0$. In this notation, the probability weight of the trajectory $\mathbf{t} = \left\{ (t_i^E, t_i^I, t_i^R) \right\}_{i=1}^N$ can be written as

$$\mathbb{P}\left[\boldsymbol{t}\right] = \prod_{i} \left[\gamma \delta\left(t_{i}^{E}\right) \delta\left(t_{i}^{I}\right) + (1 - \gamma) \Lambda\left(\sum_{j \neq i} \left[t_{j}^{I} \leq t \leq t_{j}^{R}\right] \lambda_{ji}\left(t\right), t_{i}^{E}\right) \Lambda\left(\nu_{i} \mathbb{I}\left[t_{i}^{E} \leq t\right], t_{i}^{I}\right) \right] \Lambda\left(\mu_{i} \mathbb{I}\left[t_{i}^{I} \leq t\right], t_{i}^{R}\right)$$
(B1)

Tests-based observations can be defined by generalizing the argument discussed in Section IV for the SI model. Once again, the simplest realization of test r consists in a noisy evaluation of the individual's infection state, whose outcome obeys the following stochastic expression, conditioned w.r.t. the time trajectory of individual i:

$$\mathbb{P}\left[r = + | t_i\right] = (1 - p_{FNR}) \mathbb{I}\left[t_i^E \le t < t_i^R\right] + p_{FPR}\left(\mathbb{I}\left[t < t_i^E\right] + \mathbb{I}\left[t \ge t_i^R\right]\right)$$
(B2a)

$$\mathbb{P}\left[r = -|t_i| = p_{FNR} \mathbb{I}\left[t_i^E \le t < t_i^R\right] + (1 - p_{FPR})\left(\mathbb{I}\left[t < t_i^E\right] + \mathbb{I}\left[t \ge t_i^R\right]\right)$$
(B2b)

where p_{FPR} (resp. p_{FNR}) is the false positive (resp. negative) ratio of the test. Here we implicitly assumed that the test outcome does not depend on any acquired immunity.

Finally, the definition of the risk measure Eq. (13) can be straightforwardly generalized to the SEIR model

$$\mathbb{P}\left[x_{i}\left(t\right) = I \middle| \mathcal{O}\right] = \int d\mathbf{t} \mathbb{I}\left[t_{i}^{I} \leq t < t_{i}^{R}\right] \mathbb{P}\left[\mathbf{t} \middle| \mathcal{O}\right]$$
(B3)

where $\int d\mathbf{t}$ denotes the integral over all transition time triplets $(t_1^E, t_1^I, t_1^R), \dots, (t_N^E, t_N^I, t_N^R)$.

Appendix C: Parametrization in the Causal Variational Approach

A strong advantage of CVA is its flexibility in parametrization of the ansatz solution. It is sufficient, indeed, to weakly generalize the prior model in order to obtain the form of the $Q_{\theta}(x)$ to optimize. In this section we will describe the parametrizations used for the three models whose results are presented in the main text, namely the Random Walk and the epidemic SI and SEIR models.

Random Walk – Here the generative model is a time-discrete process, where at each time the walker chooses to jump right or left with a uniform probability 1/2. As discussed in Section III of the main text, we aim at characterizing the probability distribution of a constrained random walk. The CVA simply consists in assuming a more comprehensive parametrization of the generative model, in a way that, the conditioned distribution thus obtained still describes a Random Walk, but with heterogeneous parameters. In particular, instead of fixing the jump probability to 1/2, we allow it to take diverse values, depending on time and space. So the parameters of the $Q_{\theta}(x)$ are simply the probabilities r_i^t to jump to right for a walker that at time t is in position i. Therefore, the ansatz has the following form:

$$Q_{\theta}(\mathbf{x}) = \prod_{t=0}^{T-1} \sum_{x} \left[r_x^t \delta_{x(t+1),x+1} + \left(1 - r_x^t \right) \delta_{x(t+1),x-1} \right] \delta_{x(t),x}$$
 (C1)

which is just an inhomogeneous time-dependent random walk. CVA reduces to optimize Q over the $\{r_i^t\}_{i=1,\dots,N}^{t=1,\dots,T}$. $SI \ model -$ The generative SI model is described in the main text (Eq (11)). The generative model has an infection parameter λ and a zero-patient probability γ . The Causality ansatz is obtained by generalizing these parameters. It is sufficient to introduce effective infection rates and zero-patient probabilities $\{\lambda_i\}_{i=1,\dots,N}$ and and $\{\gamma_i\}_{i=1,\dots,N}$ for each individual i, respectively. In other words, we infer the conditioned, constrained SI model with an unconditioned but inhomogenehous and time-dependent SI model. In our work, we generalized the Causal inferential model a bit further by introducing self-infection rates $\{\omega_i\}_{i=1,\dots,N}$, i.e. the rates to get infected without any contact with a positive individual. This phenomenon, of course, does not exist in the

generative model. However, it is useful to take it into account during the inference because it might help to reconstruct the infection chain. The formula for the CVA ansatz is therefore:

$$Q_{\theta}(\boldsymbol{x}) = \prod_{i} \left\{ \gamma_{i} \delta\left(t_{i}\right) + \left(1 - \gamma_{i}\right) \Lambda\left(\sum_{j \neq i} \mathbb{I}\left[t_{j}^{I} \leq t\right] \lambda_{ji}\left(t\right) + \omega_{i}\left(t\right), t_{i}\right) \right\},$$
(C2)

Notice that equation (C2) is almost identical to (11) except for the presence of self-infection. The message is that again, as in the Random Walk case, we are inferring an SI model with an SI model (with self-infection), so that the form of the ansatz is as simple as the generative distribution.

The SI model considered here is continuous in time, so that the variational parameters λ_i and ω_i should in principle be treated as continuous functions over time as well.

Since it is not possible to optimize over a function defined on a finite real domain, it is more convenient to express such rates using a family of functions, defined by a set of parameters, and optimize over the latter. A simple choice - adopted in all the results presented in the main text - is a Gaussian-like (not normalized) function for each site-dependent rate λ_i and ω_i . Each Gaussian rate will thus depend on three parameters, namely the value of the peak (labeled using μ), the standard deviation (σ), and a scale factor (p). For instance, the infection rate $\lambda_i(t)$ reads:

$$\lambda_i(t) = \lambda_i^p \exp\left[-\left(\frac{t - \lambda_i^{\mu}}{\lambda_i^{\sigma}}\right)^2\right],\tag{C3}$$

and analogous expressions hold for the self-infection rates $\omega_i(t)$ with parameters $(\omega_i^p, \omega_i^\mu, \omega_i^\sigma)$. With this choice, the total set of parameters to optimize over is given by:

$$\theta = \{\lambda_i^p, \lambda_i^\mu, \lambda_i^\sigma, \omega_i^p, \omega_i^\mu, \omega_i^\sigma, \gamma_i\}_{i=1,\dots,N}$$
 (C4)

Non-Markovian SI model – A generalized version of SI model can be obtained by allowing the infection rates to depend on the infectious status of the potential infector node. This is quite a realistic hypothesis. In fact, when an individual gets infected, its infectivity is not constant in time in real situations. Typically, infectivity is very low in a first time-window after the contagion, then it increases in the following times (typically of the order of the days), and finally it decreases to zero. In this case, the generative rate λ is no more a constant function in time, but it depends on the time elapsed since infection. The infectivity at time t of an individual t that gets infected at time t_t is therefore equal to $\lambda(t-t_t)$. Notice that λ is the same function for all the individuals. Therefore, two individuals that get infected at the same time will have the same infectivity at all times. Notice also that the generative model is Non-Markovian because in order to know the configuration at time t+dt it is not sufficient to know the state at time t, but a memory of all the infection times of each individual must be kept. Even though the generative model becomes more complex, the inference with CVA has no modifications with respect to the Markovian case. In order to make inference on this model, in fact, we use the very same parameters introduced in the Markovian SI case described above. In particular, we define:

$$\lambda_{ji}^{eff}(t|t_j) := \frac{\lambda(t - t_j)\lambda_i(t)}{\lambda_0} \tag{C5}$$

as the effective infection rate from individual j to individual i at time t given the infection time t_j (λ_0 is needed to preserve the correct dimension, but it can be numerically set to 1). We have thus defined an effective infection rate that takes into account the infectivity of j (which is given by the generative model) and the susceptibility of i to be infected (which instead is learnt by CVA). The Markovian case is obtained by setting λ to a constant and $\lambda_0 = \lambda$. The Markovian case, therefore, corresponds to the situation in which every individual in the state I has always the same probability to infect one of its contacts.

SEIR model – The SEIR is almost identical to the SI model described above. The generative model is slightly richer, with a latency rate ν and a recovery rate μ , corresponding respectively to transitions $E \to I$ and $I \to R$. Except for these two new parameters, the model of infection is equivalent to the SI. An individual in state "I" can infect a "S" individual with rate λ . Because of the similarities between the SI and the SEIR model, the parametrization of the ansatz $Q_{\theta}(x)$ is almost identical to the previous case. The parameters θ encompass, for each individual i, the zero-patient probability, an infection rate function $\lambda_i(t)$, an auto-infection rate $\omega_i(t)$, and the recovery and latency rates $\mu_i(t)$ and $\nu_i(t)$. In the results shown in Section IV of the main text, all the rates are parametrized using Gaussian functions, as in Eq. (C3).

As a final remark, it is worth noting that for both the SI and the SEIR the total number of parameters used by the CVA scales with N (in particular, their number is 7N for the SI and 13N for the SEIR).

Appendix D: Sampling in the Causal Variational Approach

Sampling from the posterior distribution is a difficult task in general. The CVA allows one to approximate the posterior with a distribution Q_{θ} from which, instead, it is possible to sample efficiently. The sampling process is crucial for performing the gradient descent described in Appendix E. For this reason this Appendix contains all the implementation details required to sample all the models implemented in the paper.

Random walk – In Appendix C we explained that the ansatz Q is an inhomogeneous time dependent random walk. Let us call $x = (x^0, x^1, \dots, x^T) \sim Q$ the trajectory, where x^t is the position of the walker at time t and $x^0 = 0$. To sample x suffices to loop over time, up to the final time T. At each temporal step we update $x^{t+1} = x^t + \Delta x$, where $\Delta x \in \{-1, +1\}$ is a binary random variable. The probability $r_{x^t}^t$ for Δx to be 1 is the probability for a walker to jump to right at time t starting from position x^t .

 $SI \ model$ — The parametrization used to infer the conditioned SI model is an SI model itself with self-infection probability, as described in Appendix C. To sample from the SI model distribution we used a Gillespie algorithm, which is described in detail in Algorithm 1. The idea behind the algorithm is to store in a queue $L = (L_1, L_2, \ldots, L_N)$ the infection times of all the individuals. To this end, the first step consists in sampling all the zero-patient(s), i.e. all individuals i such that $L_i = 0$. Secondly, we sample self-infection events for each non zero-patient individual i, with a random variable t_i extracted from the self-infection distribution $\omega_i(t)$.

Finally, contagion events are sampled by extracting from the queue the individual having the minimum value of L. If an individual i tries to infect another individual j at time t_{ij} , then j updates its infection time by taking the minimum between t_{ij} and its current value of L_j . In this way the list is updated recursively. As a final remark, notice that to ensure a proper epidemic process to take place, at least one zero patient is needed. Therefore, it is necessary to sample events with $L_i = 0$ by constraining a positive number n_{zp} of zero-patients. This procedure can be easily carried out recursively. For instance, starting from node 1, we set it to be a patient-zero with probability:

$$\mathbb{P}(L_1 = 0 | n_{zp} > 0) = \frac{\mathbb{P}(L_1 = 0, n_{zp} > 0)}{\mathbb{P}(n_{zp} > 0)} = \frac{\mathbb{P}(L_1 = 0)}{\mathbb{P}(n_{zp} > 0)} = \frac{\gamma_1}{1 - \prod_{i=1}^{N} (1 - \gamma_i)}$$
(D1)

Then, the next node (say number 2) is set to be infected at t = 0 with a probability depending on L_1 , namely:

$$\mathbb{P}(L_2 = 0 | L_1, n_{zp} > 0) = \begin{cases} \gamma_2 & \text{if } L_1 = 0\\ \gamma_2 / \left(1 - \prod_{i \ge 2} (1 - \gamma_i)\right) & \text{if } L_1 > 0 \end{cases}$$
 (D2)

and the above strategy is iterated for every L_k . Intuitively, from Eq. (D2) it follows that as soon as one zero patient is sampled, the remaining individuals' state is extracted independently with probability γ_i .

Algorithm 1 Sampling the effective (Non-Markovian) SI model

- ullet Initialize a queue L
- Loop over population: $i:1,\ldots,N$
 - $-L[i] \leftarrow 0$ with probability $\gamma_i / \left(1 \prod_{j \geq i} (1 \gamma_j)\right)$
 - if L[i] = 0 break the loop
- Loop over the remaining population:
 - $-L[i] \leftarrow 0$ with probability γ_i
- Loop over the non zero-patients (variable of the loop: i)
 - $-L[i] \leftarrow t_i$ where t_i is extracted from the self-infection rate ω_i
- Loop over the queue L entering by infection time (from the smallest to the highest)
 - Call i the element extracted from L
 - **Loop** over $j \in \partial i$
 - * Extract the time t_{ij} at which i tries to infect j by extracting from the Gaussian distribution of λ_{ij}^{eff}
 - * $L[j] \leftarrow \min\{L[j], t_{ij}\}$
 - Throw away i from the queue L and save L[i] as the infection time of i.
- Return the list of infection times.

SEIR model – For the SEIR model, the sampling procedure is a straightforward generalization on the one just discussed. The only difference is that now the queue will contain all the transition time triplets t_i^E, t_i^I, t_i^R for each individual.

Appendix E: The Causal Variational Approach: Gradient Descent

In the Causal Variational Approach) the parameters θ of the approximation are determined by minimizing the following KL divergence:

$$D_{KL}(Q_{\theta}||\mathbb{P}\left[\boldsymbol{x}|\mathcal{O}\right]) = \int d\boldsymbol{x} Q_{\theta}\left(\boldsymbol{x}\right) \log\left(\frac{Q_{\theta}(\boldsymbol{x})}{\mathbb{P}\left[\boldsymbol{x}|\mathcal{O}\right]}\right), \tag{E1}$$

where Q_{θ} denotes the Causality ansatz. The integration is formal. If $\mathbb{P}[x|\mathcal{O}]$ is continuous, then it corresponds to a Lebesgue integral, otherwise it is a sum over the discrete state x.

Gradient Descent – The KL divergence can be minimized by performing a gradient descent in the θ parameter space. The parameters at iteration k+1 read

$$\theta^{(k+1)} = \theta^{(k)} - \epsilon \nabla_{\theta} D_{KL}(Q_{\theta} || \mathbb{P}[\mathbf{x} | \mathcal{O}])$$
(E2)

where ϵ is the learning rate. Before entering the calculation of the gradient, however, let us observe that, in general, θ contains parameters which have different scales, and, therefore, a straightforward implementation of Eq. E2 may be inefficient. To solve this issue, we resort to a sign descender method [9], a simple scale-free descender. Briefly, it consists in moving in the direction of the partial derivative with respect to each parameter without using the information of the gradient's magnitude.

Finally, the update rule for a parameter θ_i used in this work, has the following expression:

$$\theta_i^{(k+1)} = \theta_i^{(k)} \left[1 - \varepsilon \operatorname{sign} \left(\partial_{\theta_i} D_{KL}(Q_{\theta} || \mathbb{P} \left[\boldsymbol{x} | \mathcal{O} \right] \right) \right) \right]$$
 (E3)

We now proceed to evaluate the derivatives of the $D_{KL}(Q_{\theta}||\mathbb{P}[\boldsymbol{x}|\mathcal{O}])$.

$$\partial_{\theta_{i}} D_{KL}(Q_{\theta}||\mathbb{P}[\boldsymbol{x}|\mathcal{O}]) = \partial_{\theta_{i}} \int d\boldsymbol{x} Q_{\theta}(\boldsymbol{x}) \log \frac{Q_{\theta}(\boldsymbol{x})}{\mathbb{P}[\boldsymbol{x}|\mathcal{O}]} =$$

$$= \partial_{\theta_{i}} \int d\boldsymbol{x} Q_{\theta}(\boldsymbol{x}) \log \frac{Q_{\theta}(\boldsymbol{x})\mathbb{P}[\mathcal{O}]}{\mathbb{P}[\boldsymbol{x}]\mathbb{P}[\mathcal{O}|\boldsymbol{x}]} =$$

$$= \int d\boldsymbol{x} \partial_{\theta_{i}} \left(Q_{\theta}(\boldsymbol{x}) \log \frac{Q_{\theta}(\boldsymbol{x})}{\mathbb{P}[\boldsymbol{x}]\mathbb{P}[\mathcal{O}|\boldsymbol{x}]} \right) + \log \mathbb{P}[\mathcal{O}] \partial_{\theta_{i}} \int d\boldsymbol{x} \left(Q_{\theta}(\boldsymbol{x}) \right) =$$

$$= \int d\boldsymbol{x} \partial_{\theta_{i}} \left(Q_{\theta}(\boldsymbol{x}) \log \frac{Q_{\theta}(\boldsymbol{x})}{\mathbb{P}[\boldsymbol{x}]\mathbb{P}[\mathcal{O}|\boldsymbol{x}]} \right)$$
(E4)

in which we neglected the dependency on $P(\mathcal{O})$. We observe that

$$\int d\boldsymbol{x} \, \partial_{\theta_i} \left(Q_{\theta}(\boldsymbol{x}) \log Q_{\theta}(\boldsymbol{x}) \right) = \int d\boldsymbol{x} \, \partial_{\theta_i} Q_{\theta}(\boldsymbol{x}) \log Q_{\theta}(\boldsymbol{x}) + \int d\boldsymbol{x} \, Q_{\theta}(\boldsymbol{x}) \partial_{\theta_i} \log Q_{\theta}(\boldsymbol{x}) \tag{E5}$$

In the above expression, the second term of the r.h.s. is 0, in fact:

$$\int d\mathbf{x} Q_{\theta}(\mathbf{x}) \partial_{\theta_i} \log Q_{\theta}(\mathbf{x}) = \int d\mathbf{x} \partial_{\theta_i} Q_{\theta}(\mathbf{x}) = \partial_{\theta_i} \int d\mathbf{x} Q_{\theta}(\mathbf{x}) = 0$$
 (E6)

Finally

$$\int d\boldsymbol{x} \partial_{\theta_{i}} (Q_{\theta}(\boldsymbol{x}) \log Q_{\theta}(\boldsymbol{x})) = \int d\boldsymbol{x} (\partial_{\theta_{i}} Q_{\theta}(\boldsymbol{x})) \log Q_{\theta}(\boldsymbol{x})
= \int d\boldsymbol{x} \frac{Q_{\theta}(\boldsymbol{x})}{Q_{\theta}(\boldsymbol{x})} (\partial_{\theta_{i}} Q_{\theta}(\boldsymbol{x})) \log Q_{\theta}(\boldsymbol{x}) =
= \int d\boldsymbol{x} Q_{\theta}(\boldsymbol{x}) (\partial_{\theta_{i}} \log Q_{\theta}(\boldsymbol{x})) \log Q_{\theta}(\boldsymbol{x}) =
= \langle \log Q_{\theta}(\boldsymbol{x}) \partial_{\theta_{i}} \log Q_{\theta}(\boldsymbol{x}) \rangle_{Q_{\theta}}$$
(E7)

Finally we have the derivative of the KL divergence:

$$\partial_{\theta_{i}} D_{KL}(Q_{\theta} || \mathbb{P}[\mathbf{x} | \mathcal{O}]) = \left\langle \log \frac{Q_{\theta}(\mathbf{x})}{\mathbb{P}[\mathbf{x}] \mathbb{P}[\mathcal{O} | \mathbf{x}]} \partial_{\theta_{i}} \log Q_{\theta}(\mathbf{x}) \right\rangle_{Q_{\theta}}$$
(E8)

Now the problem of calculating the derivative of the KL divergence has been reduced to calculate the derivative of the logarithm of the ansatz and then to average over the ansatz. In principle, one may need to calculate

$$\partial_{\theta_i} \log Q_{\theta}(\boldsymbol{x}) = \sum_{j=1}^{N} \partial_{\theta_i} \log q_j(x_j, x_{\partial j})$$
 (E9)

but it is reasonable to assume that the dependency of each parameter θ_i occurs only on the term $\log q_i$. This hypothesis is true for all the examples we treated in this work, as described in the previous Appendix. Therefore

$$\partial_{\theta_i} D_{KL}(Q_{\theta} || \mathbb{P}[\boldsymbol{x} | \mathcal{O}]) = \left\langle \log \frac{Q_{\theta}(\boldsymbol{x})}{\mathbb{P}[\boldsymbol{x}] \mathbb{P}[\mathcal{O} | \boldsymbol{x}]} \partial_{\theta_i} \log q_i(x_i, x_{\partial i}) \right\rangle_{Q_{\theta}}$$
(E10)

Averages are evaluated by sampling from Q_{θ} using the implementation details given in Appendix D. The learning process is therefore the following:

- 1. The parameters are initialized to θ^0 (we initialize them with the values of the generative model, where known. For example, in the random walk example the jump probabilities are all initialized to 1/2).
- 2. The derivatives of the KL divergence are performed by sampling from Q_{θ_0} and through Eq. (E10).
- 3. The parameters are updated to θ^1 by using (E3).
- 4. Steps 2. and 3. are repeated.
- In the evaluation of the KL divergence (or its derivatives), it is necessary to evaluate quantities that include

5. The process stops when $D_{KL}(Q_{\theta}||\mathbb{P}[\mathbf{x}|\mathcal{O}])$ does not significantly change after two consecutive iterations.

 $\log \mathbb{P}(\mathcal{O} \mid x)$. When \mathcal{O} imposes a hard constraint on the trajectory - as it happens in the epidemic models with noiseless observations - the violation of one of the constraints (which is likely to occur especially in the first stages of the gradient descent) would result in $\log \mathbb{P}(\mathcal{O} \mid x) \to -\infty$. To avoid this issue, it is convenient to relax (soften) all the constraints: a small acceptance $p \sim 10^{-10}$ is introduced, in such way that $\log \mathbb{P}(\mathcal{O} \mid \boldsymbol{x})$ has always non-diverging values. As a consequence, the distribution $Q_{\theta}(x)$ resulting from the KL minimization gives a non-zero (yet very small) probability to events x which do not satisfy the constraint.

Appendix F: Inference of Hyperparameters

As explained in Section IV in the main text, the term hyperparameters refers to parameters of a generative model. For example, the Random Walk presented in Section III has a unique hyperparameter, namely the probability of a right jump, which is set to 1/2 for all times and sites. In the SI model, the hyperparameters are the zero-patient probability γ and the infection rate λ while in the SEIR model we need to add to the hyperparameters set the latency rate ν and the recovery rate μ . Usually, in inference problems, they are not known as the only source of information, in fact, are the observations. However, inferring the hyperparameters from observations is crucial to ensure an effective solution to the underlying inference problem. The CVA allows one to estimate them. Let us call the set of hyperparameters θ^p . First, notice that in general not only the generating distribution $\mathbb{P}[x]$, but also the ansatz Q_{θ} depends on the hyperparameters θ^{p} . The dependency on Q_{θ} might be present when we use part of the generative model in the ansatz distribution. The example implemented in this paper is the case of Non-Markovian SI model (see Appendix C). In that case, the infectivity function depends on both the inferred parameters $\{\lambda_i\}\in\theta$ and the relative infectivity of the generative model $(\lambda \in \theta^p)$, as shown in Eq. (C5). Thus, the KL divergence depends on θ^p through both Q_θ and $\mathbb{P}[x]$, so that in the following the notation $Q_{\theta,\theta_p}=Q_{\theta_p}$, $\mathbb{P}=\mathbb{P}_{\theta_p}$ is used for sake of simplicity. As it happens for the parameters of the variational ansatz, the hyperparameters can be inferred through a gradient-descent. The derivative of the KL with respect one hyperparameter, denoted with θ_i^p , is given by:

$$\partial_{\theta_{i}^{p}} D_{KL}(Q_{\theta^{p}} || \mathbb{P}_{\theta^{p}}) = \partial_{\theta_{i}^{p}} \int d\mathbf{x} \, Q_{\theta^{p}}(\mathbf{x}) \left(\log \frac{Q_{\theta^{p}}(\mathbf{x})}{\mathbb{P}_{\theta^{p}}[\mathbf{x}] \, \mathbb{P}[\mathcal{O} | \mathbf{x}]} + \log \mathbb{P}[\mathcal{O}] \right) =$$

$$= \partial_{\theta_{i}^{p}} \left\langle \log \frac{Q_{\theta^{p}}(\mathbf{x})}{\mathbb{P}_{\theta^{p}}[\mathbf{x}] \, \mathbb{P}[\mathcal{O} | \mathbf{x}]} \right\rangle_{Q_{\theta^{p}}} + \partial_{\theta_{i}^{p}} \log \mathbb{P}[\mathcal{O}] =$$

$$= \partial_{\theta_{i}^{p}} \left\langle \log \frac{Q_{\theta^{p}}(\mathbf{x})}{\mathbb{P}_{\theta^{p}}[\mathbf{x}] \, \mathbb{P}[\mathcal{O} | \mathbf{x}]} \right\rangle_{Q_{\theta^{p}}}.$$
(F1)

Up to now, the above expression is identical to Eq. (E4), with the difference that now also \mathbb{P} depends on θ^p . Using the trick of Eq. (E7), i.e. that $\langle \partial_{\theta^p} \log Q \rangle_{Q_{\theta^p}} = 0$, we get:

$$\partial_{\theta_{i}^{p}} D_{KL}(Q_{\theta^{p}}||\mathbb{P}_{\theta^{p}}) = \left\langle \log \frac{Q_{\theta^{p}}(\boldsymbol{x})}{\mathbb{P}_{\theta^{p}}[\boldsymbol{x}] \mathbb{P}[\mathcal{O}|\boldsymbol{x}]} \left(\partial_{\theta_{i}^{p}} \log \frac{Q_{\theta^{p}}(\boldsymbol{x})}{\mathbb{P}_{\theta^{p}}[\boldsymbol{x}]} \right) \right\rangle_{Q_{\theta^{p}}} = \\
= \left\langle \log \frac{Q_{\theta^{p}}(\boldsymbol{x})}{\mathbb{P}_{\theta^{p}}[\boldsymbol{x}] \mathbb{P}[\mathcal{O}|\boldsymbol{x}]} \partial_{\theta_{i}^{p}} \log Q_{\theta^{p}}(\boldsymbol{x}) \right\rangle_{Q_{\theta^{p}}} - \left\langle \log \frac{Q_{\theta^{p}}(\boldsymbol{x})}{\mathbb{P}_{\theta^{p}}[\boldsymbol{x}] \mathbb{P}[\mathcal{O}|\boldsymbol{x}]} \partial_{\theta_{i}^{p}} \log \mathbb{P}_{\theta^{p}}[\boldsymbol{x}] \right\rangle_{Q_{\theta^{p}}}. (F2)$$

The above equation is the equivalent of Eq. (E8) in case of hyperparameters learning. The first term is identical in form to (E8), while the second arises because also the generative model depends on the hyperparameters. Apart on this difference, the learning process for θ^p is identical to learning θ : we calculate the averages in r.h.s of Eq. (F2) by sampling and then we update the hyperparameters using the Sign Descender rule. From an computational point of view, we chose to update both the paramers θ and the hyperparameters θ^p at each iteration.

Appendix G: Other Inferential Methods

This section provides a brief description of the several inferential techniques whose performances are compared in Section IV.

Sib – This method is based on a Belief Propagation approach to epidemic spreading processes, that allows one to compute, in an efficient and distributed way, the marginals over a posterior distribution (Eq. (1)) for compartmental epidemic models with non-reccurrent dynamics (eventually non-Markovian). It shows very good performances for random contact networks, while it suffers the presence of loops in the graph. A detailed explanation of this method can be found in [1].

Mean Field (MF) – This method is based on a heuristic way to deal with clinical test based observations, and on a Mean Field approximation of the prior distribution, which is considered to be factorized over nodes at each time. An advantage of this method relies on its simplicity and small computational cost; however, it typically shows poorer performances with respect to the other methods. We refer to [1] for additional details about the MF approximation. The heuristic scheme is instead discussed in the next paragraph.

Heuristic (heu) – The MF method developed in [1] and described above relies on two approximations. The first is a heuristic way to deal with observations: it consists in assuming that if an individual is tested positive at time t, then it became positive at time $t-\tau$, with τ properly tuned (to further details we refer to [1]). The second is a MF ansatz for the prior distribution. It is natural to ask whether such a heuristic is a good approximation for the observation constraints, regardless of the MF factorization ansatz. We therefore replace the MF estimation of marginal probabilities by sampling trajectories forward in time. As shown in Section IV, this method always shows better performances w.r.t. MF. The heuristic, therefore, is a good guess for epidemic risk assessment.

As a final remark, the Causal Variational Approach can actually be considered as a further extension of the MF approximation [1] in the following sense:

- 1. it gives a full justification to the heuristic using a variational principle.
- 2. it extends [1] by allowing the patient zero inference.
- 3. it allows one to infer the hyperparameters of the generative model and to perform epidemic reconstruction in the case of a non-Markovian dynamics.

Soft-Margin – The Soft-Margin estimator is described in [4]. We developed the method by sampling from the prior probability distribution and weighting each sample with the observation probability. The technique is asymptotically exact. However, when the population size grows, the probability to sample a trajectory which satisfies the observation constraints dramatically decreases. Therefore, we expect the method to be quite slow for large population size in order to well-approximate the posterior distribution.

Appendix H: Models of contact networks used in the numerical simulations

Proximity model – The proximity contact graph is obtained distributing N individuals uniformly in a square of side \sqrt{N} and generating the contacts as follows. A contact can be established between two individuals i and j with a probability $e^{-d_{ij}/\ell}$, where d_{ij} is the Euclidean distance between the points i and j are located and ℓ is a length scale that can be tuned to change the density of the contact graph.

Spatio-temporal model from geolocation data – Dynamic contact network instances with realistic patterns of time-dependent contacts can be generated using the spatio-temporal model in Ref. [6]. According to this model, individuals are assigned to households that are localized on a urban area according to the actual population density. Other venues (schools and research institutes, social places, bus stops, workplaces, and supermarkets) are similarly displaced in the map according to available geo-location data. In a mobility simulation, individuals can visit a certain number of locations with a probability that decreases as the household-target distance increases. The duration of contacts between individuals concurrently visiting the same venue is assumed to be known and gathered by contact tracing smart-phone applications. Some interesting and realistic features naturally arise from this contact dynamics, such as the presence of super-spreaders, e.g. the number of infections caused by infectious individuals is over-dispersed. In the present work, only a small example of such kind of dynamically generated contact network was analyzed. The contact-network instances used to obtain results in Fig. 3 represent the interaction graph among a small community of N = 904 individuals moving on a coarse-grained version of the city of Tübingen, in Germany. Due to the rescaling of the population, also the number of venues in the urban area was rescaled by a factor of 20.